Korean J. Chem. Eng., **21**(1), 221-229 (2004)

Effects of Charge Density on Water Splitting at Cation-Exchange Membrane Surface in the Over-Limiting Current Region

Moon-Sung Kang, Yong-Jin Choi and Seung-Hyeon Moon†

Department of Environmental Science and Engineering, Kwangju Institute of Science & Technology (K-JIST), 1 Oryong-dong, Buk-gu, Gwangju 500-712, South Korea
(*Received 1 July 2003 • accepted 20 October 2003*)

Abstract−To determine the correlation between surface properties and concentration polarization (CP) behaviors, cation exchange membranes with varying fixed charge densities were prepared and characterized by using several electrochemical analyses such as chronopotentiometry, zeta potential, and current-voltage measurements. Results showed that CP behavior depended mainly on surface charge density. With higher surface charge density, stronger electroconvection was observed, suggesting that an increase in the surface charge density increased the concentration of the counter ions at the membrane surface. As such, the electric field around the membrane surface was strengthened at a current over the limiting current density. Water splitting was also proportional to the surface charge density. This result was consistent with the classical electric field-enhanced water splitting theory, indicating that water splitting increased due to increases in the electric field and prepolarization of water molecules at the membrane-solution interface of the cation-exchange membrane.

Key words: Cation-Exchange Membranes, Surface Charge Density, Concentration Polarization, Water Splitting, Electric Field

INTRODUCTION

For the past decades, much attention has been given to electrically driven processes (*e.g.*, electrodialysis, water-splitting electrodialysis, and electrodeionization) using ion-exchange membranes (IEMs) for the desalination of seawater [Melnik et al., 1999; Shi and Chen, 1983], separation of amino acids [Kang et al., 2002a; Kim and Moon, 2001; Lee et al., 2002; Minagawa et al., 1997; Montiel et al., 1998; Sato et al., 1995], and other purposes [Kang et al., 2002b; Paleologou et al., 1996; Shaposhnik and Kesore, 1997]. Since IEMs play an important role in these processes, the ion transport phenomena through an IEM should be understood to enhance the process efficiency.

Concentration polarization (CP) is one of the most important phenomena in the IEM processes. CP occurs at the interface between a membrane and an electrolyte solution when current is applied. Since this phenomenon causes significant problems in electro-membrane processes including water splitting (WS) and increase in power consumption, it has been studied extensively for many years [Choi et al., 2001a; Kang et al., 2003; Krol et al., 1999; Rubinstein et al., 1988; Simons, 1979]. It has been widely accepted that the nature of the membrane influences CP only through permselectivity. In practice, however, different membranes with the same permselectivity exhibit individual unique CP behaviors and water splitting capabilities [Rubinstein et al., 1988]. The findings clearly indicate that the membrane surface plays an important role in polarization phenomena.

The membrane properties contributing to the polarization phenomena in ion-exchange membranes include: (i) ionic permselectivity; (ii) surface morphology; (iii) type of fixed charge groups; (iv) distribution or concentration of fixed charge groups, and; (v) nature of membrane material (*e.g.*, hydrophilicity). These parameters may affect the formation of electric fields around IEMs and result in diverse CP behaviors. Rubinstein et al. [1988] reported that polarization behaviors are substantially different for membranes of different composition, even under the identical flow conditions. The limiting current densities (LCDs) for an ideally permselective homogeneous membrane were particularly lower than the expected theoretical values. This implies that a non-conducting area exists on the membrane surface. The lack of conductive homogeneity on the membrane surface is expected to yield a strongly non-uniform electric field promoting the over-limiting current. Meanwhile, Krol et al. [1999] confirmed the existence of non-conducting areas on the membrane surface by measuring the transition time (τ) in chronopotentiometry. More recently, Choi et al. [2001b] suggested a method for quantitatively estimating the fraction of the conducting region (ε_c) on the ion-exchange membrane surface by using the modified Sand equation. Results of the studies showed that surface heterogeneity is an intrinsic property of ion-exchange membranes. Nonetheless, the interrelationship between surface conductive-heterogeneity and ion-transport phenomena in the over-limiting current region has not been systematically investigated yet. Furthermore, the effects of such membrane surface properties on water splitting have not been clearly explained.

This study aimed to investigate the role of solution-membrane interface in concentration polarization and water splitting behaviors in the over-limiting current region. Results of this study may provide useful information for the over-limiting current operation of electro-membrane processes and for the design of ion-exchange

†To whom correspondence should be addressed.
E-mail: shmoon@kjist.ac.kr
‡This paper is dedicated to Professor Hyun-Ku Rhee on the occasion of his retirement from Seoul National University.

membranes that can be utilized in a high current condition. For this study, sulfonated poly(arylene ether sulfone) (S-PES) cation-exchange membranes with varying fixed charge densities were prepared and their electrochemical and surface properties characterized. Since the analysis of the anion-exchange membrane was complicated due to the chemical changes in quaternary ammonium groups in the over-limiting current region that triggers violent water splitting, this study was limited only to the case of a cation-exchange membrane.

EXPERIMENTAL

1. Preparation of S-PES Cation Exchange Membranes

Sulfonated poly(arylene ether sulfone) (S-PES) membranes were prepared by using the direct polymerization route as shown in Fig. 1 [Mecham et al., 2000; Wang et al., 2002]. Sulfonated 4,4'-dichlorodiphenylsulfone (S-DCDPS) monomers were synthesized and subsequently polymerized with 4,4'-biphenol and 4,4'-dichloro diphenylsulfone (DCDPS) monomers. All reagents were purchased from Aldrich Chemical Company. The polymerization solvent *N*-methyl-2-pyrrolidone (NMP) was distilled from phosphorous pentoxide under a vacuum prior to use.

S-PES membranes with different degrees of sulfonation were made by varying the molar ratio of S-DCDPS to the total amount of monomers added. Selected molar ratios (S-DCDPS/(S-DCDPS+DCDPS)) were 20, 30, 40, 50, and 60 mol%. After the synthesis of the sulfonated polymers, the membranes were prepared by casting viscous 30 wt% S-PES/NMP solutions onto clean glass plates. The glass plates were then placed in a vacuum oven at 80 °C for 6 hrs, with the temperature increased stepwise to 140 °C for 2 hrs, 220 °C for another 2 hrs, and 300 °C for an hour to remove residual solvent completely. The membranes were thoroughly rinsed with distilled water and subsequently stored in a 0.50 mol dm^{-3} NaCl solution for more than a day.

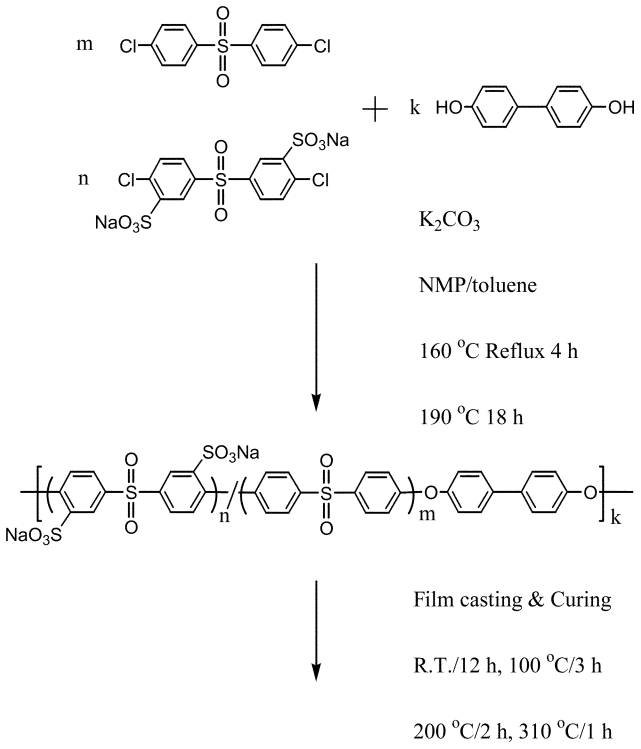

Fig. 1. Polymerization scheme for sulfonated poly(arylene ether sulfone) (S-PES).

Several types of commercial cation-exchange membranes were also characterized for reference. Neosepta® CM-1, CMX, and CMB membranes were purchased from Tokuyama Corp. (Japan). A heterogeneous type of cation exchange membrane listed as HQC was purchased from Hangzhou Qianqiu Chemical (China).

2. Evaluation of Membrane Properties

The water content, electrical resistance, ion-exchange capacity, and apparent transport number for the counter ion were determined. Chronopotentiometric and current-voltage (I-V)/current-resistance (I-R) curves were also obtained from two-compartment cell experiments. Detailed experimental procedures were described in previous studies [Choi et al., 2001a; Choi and Moon, 2001; Kang et al., 2002a, 2003].

The zeta potential values of membrane surface were determined through electrophoretic mobility measurements with an electrophoresis measurement apparatus (ELS-8000, Photal, Otsuka Electronics, Japan) with a plate sample cell [Shim et al., 2002]. Polystyrene latex particles (520 nm diameter; Otsuka Electronics, Japan) coated with hydroxy propyl cellulose having an average molecular weight of 300,000 (Scientific Polymer Products, Japan) were used as standard monitoring particles. These were dispersed in a 0.01 mol dm^{-3} NaCl solution to prevent interactions with or adsorption on the quartz cell surface during measurements. Water-splitting capabilities were determined by using six-compartment cell experiments [Kang et al., 2002a]. The transport number of water ions (H^+ and OH^-) in the membrane was calculated from the change in pH according to:

$$t_{H^+} = \frac{FV(\Delta C_{H^+}/\Delta t)}{IA} = t_{OH^-} = \frac{FV(\Delta C_{OH^-}/\Delta t)}{IA}, \quad (1)$$

where V is the volume of the solution, F the Faraday constant, $C_{H+/OH-}$ the concentration of proton/hyroxyl ion, t the time, I the current density, and A the membrane area.

RESULTS AND DISCUSSION

1. Effects of Membrane Surface Properties on Concentration Polarization (CP)

Chronopotentiometry is an effective tool for investigating mass transfer at the membrane-solution interface [Choi et al., 2001b; Krol et al., 1999]. In this study, the fraction of the conducting region ε_c for each ion-exchange membrane was determined by using the modified Sand equation proposed by Choi et al. [2001b]:

$$\varepsilon_c = \frac{2i\tau^{1/2}(\bar{t}_k - t_k)}{C_o z_k F(\pi D)^{1/2}}, \quad (2)$$

where ε_c is the fraction of conducting region, i the current density, τ the transition time, C_o the concentration of electrolyte, z_k the valence of k ion, F the Faraday constant, and D the diffusion coefficient of electrolyte. $\bar{t}_k$, t_k are the transport numbers of k ion in the membrane and solution phases, respectively. Fig. 2 shows the chronopotentiometric curves for each membrane at a constant current density (25.0 A m^{-2}). The transition time (τ) was determined by using the intersection of the tangents with the first and second stages of the curve. For the calculation of the ε_c values, the diffusion coef-

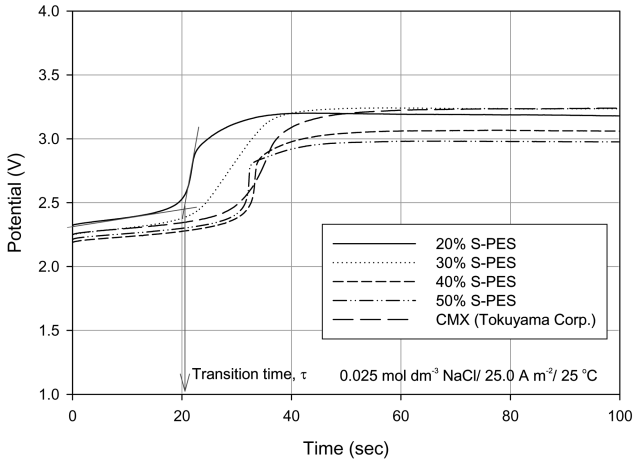

Fig. 2. Chronopotentiometry curves for determining the surface heterogeneity of IEMs.

ficient (1.61×10^{-5} cm^2 sec^{-1}) of NaCl and the transport number (0.396) of Na^+ ion in the solution phase were obtained from literature [Crow, 1994]. By incorporating the apparent transport numbers for each membrane into Eq. (2), the ε_c values were calculated.

Table 1 lists various membrane properties including water content, ion-exchange capacity (IEC), apparent transport number, electrical resistance, and fraction of surface conducting region. With an increase in the percentage of sulfonated monomers (S-DCDPS), the water content and IEC of the S-PES membranes increased while the electrical resistances decreased. The apparent transport numbers were maintained at greater than 0.98 (for Na^+) for all samples.

Table 2. Zeta potentials of the S-PES membranes (in 0.010 mol dm^{-3} NaCl/ electrophoretic measurement)

Membranes	20% S-PES	30% S-PES	40% S-PES	50% S-PES
Zeta potential (mV)	−4.35	−7.16	−14.35	−17.98

As expected, the ε_c values of the S-PES membranes increased with an increase in the number of sulfonic acid groups. Results showed that as the fixed charge density increased, conductive homogeneity was also enhanced.

Table 2 lists the apparent zeta potentials on the membrane surface. The zeta potential measurements were repeated several times to ensure reproducibility. The apparent zeta potential values negatively increased according to the increase in the number of sulfonic acid groups, thus indicating an increase in the surface charge density. The apparent surface charge densities (σ_s) of the membrane were also calculated from the zeta potential values by using the Gouy-Chapman equation [Jimbo et al., 1999]:

$$\sigma_s = \frac{2\varepsilon_0\varepsilon_r kT\kappa}{ze}\sinh\left(\frac{ze\zeta}{2kT}\right), \quad (3)$$

where ζ is the zeta potential, k the Boltzmann constant, T the temperature, κ the reciprocal of the Debye screening length, ε_r the relative permittivity, ε_0 the vacuum electric permittivity, z the valency of the counter ion, and e the coulombic charge. The apparent surface charge densities measured in a 10 mmol dm^{-3} NaCl varied from −0.10 to −0.42 μC cm^{-2} according to the IEC (*i.e.*, 1.13-2.12 meq. g^{-1}) of the S-PES membranes as shown in Fig. 3. The increases (in negative direction) in the measured surface charge density corre-

Table 1. Evaluated basic membrane properties

(a) S-PES membranes

Membranes	20% S-PES	30% S-PES	40% S-PES	50% S-PES
Water content (-)	0.084	0.123	0.228	0.284
Ion exchange capacity (meq./g)	1.13	1.48	1.86	2.12
Electrical resistance (Ω cm^2)	7.24	1.65	0.98	0.77
Transition time, τ (sec)	20.57	22.55	32.45	31.79
$I\tau^{1/2}$	11.34	11.87	14.24	14.10
Transport no. (-)*	1.152	1.118	0.998	1.000
Transport no. (-)**	0.998	0.993	0.987	0.994
Fraction of conducting region, ε_c (-)	0.796	0.826	0.981	0.983

(b) Commercial membranes

Membranes	CM-1	CMX	CMB	HQC
Water content (-)	0.36	0.27	0.43	0.45
Ion exchange capacity (meq./g)	2.26	1.67	3.11	1.79
Electrical resistance (Ω cm^2)	1.27	2.98	3.42	4.69
Transition time, τ (sec)	22.31	21.31	20.09	20.75
$I\tau^{1/2}$	14.17	13.85	13.45	13.67
Transport no. (-)*	1.001	1.015	1.034	1.024
Transport no. (-)**	0.985	0.987	0.980	0.915
Fraction of conducting region, ε_c (-)	0.973	0.954	0.916	0.827

*measured by chronopotentiometry.

**measured by emf method.

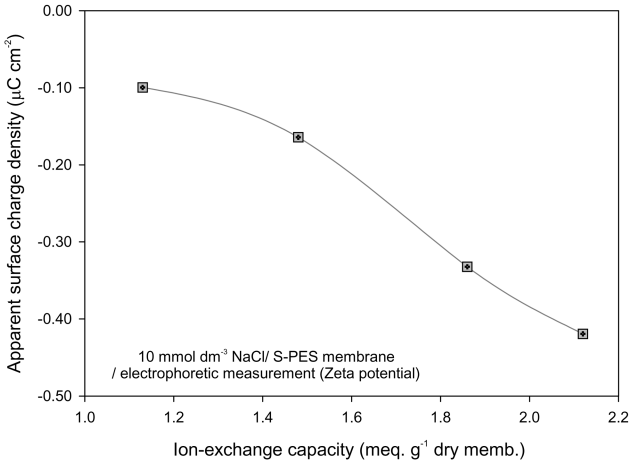

Fig. 3. Apparent surface charge densities according to the ion-exchange capacity (S-PES membranes).

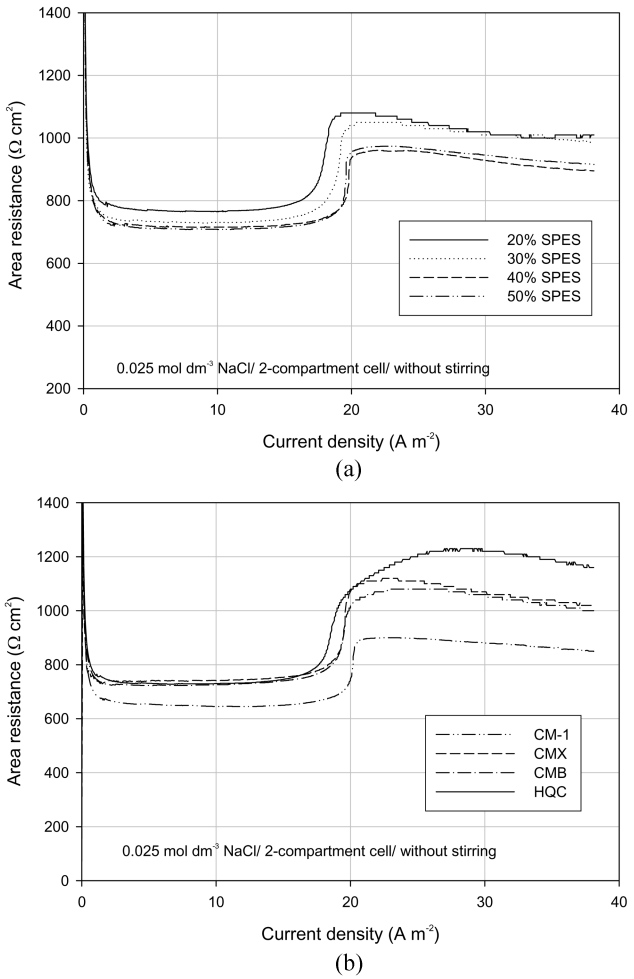

Fig. 4. Current-resistance (I-R) curves of cation-exchange membranes.
(a) S-PES membranes; (b) Commercial membranes

sponded with the increases in the ε_c values suggested in Table 1.

The specific membrane properties of the selected commercial membranes are also reported in Table 1(b). The ε_c value for CM-1 was highest among the commercial membranes. In cases where the membranes had excellent mechanical strength (*i.e.*, CMX, CMB, and HQC) since reinforcing materials such as poly(vinyl chloride) (PVC) powder, might be introduced in abundance, the heterogeneity of the surface increased. The fractions of conducting regions in each membrane increased in the following order: HQC<CMB<CMX <CM-1.

Table 3. Characteristic values of I-R curves (S-PES and commercial membranes)

(a) S-PES membranes

Membranes	20% S-PES	30% S-PES	40% S-PES	50% S-PES
R_{1st} (Ω cm^2)	766.9	737.0	718.4	714.6
R_{3rd} (Ω cm^2)	1032.5	989.4	929.5	921.1
R_{3rd}/R_{1st} (-)	1.346	1.343	1.294	1.289
$R_{inc.}$ (%)	34.6	34.3	29.4	28.9
ΔR (Ω cm^2)	265.6	252.4	211.1	206.4
LCD (A m^{-2})	17.3	18.4	19.5	19.3

(b) Commercial membranes

Membranes	CM-1	CMX	CMB	HQC
R_{1st} (Ω cm^2)	650.0	746.0	730.2	733.1
R_{3rd} (Ω cm^2)	878.7	1072.6	1051.0	1201.0
R_{3rd}/R_{1st} (-)	1.352	1.438	1.439	1.638
$R_{inc.}$ (%)	35.2	43.8	43.9	63.8
ΔR (Ω cm^2)	228.7	326.6	320.8	467.9
LCD (A m^{-2})	20.0	19.4	19.1	17.0

Fig. 4 shows the current-resistance (I-R) relations for the cation-exchange membranes investigated in this study. Markedly different I-R curves representing different CP behaviors were observed for the different membranes. Table 3 summarizes the characteristic values of the curves. The electrical resistances in the Ohmic region under the LCD (*i.e.* R_{1st}) decreased with increase in the IEC. This indicated that the R_{1st} strongly depended on membrane conductivity. The difference in resistances at, under, and over the LCD (R_{3rd}-R_{1st}, ΔR) and the resistance ratio (R_{3rd}/R_{1st}) also indicated varying CP behaviors [Choi et al., 2001a]. The parameters were obtained by using graphic software (*i.e.* Origin®7.0, OriginLab Corp., USA). The ΔR values representing energy requirements for destroying the diffusion boundary layer (like plateau length (ΔV) in I-V curve)) decreased with an increase in the fraction of surface conducting region and the ion exchange capacity. The R_{3rd}/R_{1st} values also showed the same trends, indicating that increasing the fixed charge density on the membrane surface strengthened the electro-convective force in the over-limiting current region [Choi et al., 2001a].

Electroconvection has been understood as a phenomenon triggered by a strongly non-uniform electric field resulting from a lack in conductive homogeneity on a membrane surface over the LCD [Krol et al., 1999; Rubinstein, 1991; Rubinstein et al., 1997]. The non-uniform electric field may be induced by the existence of non-conducting regions on the membrane surface or microscopic non-uniform distributions of the fixed charge groups. According to the theory, the lack of surface homogeneity formed by the existence of non-conducting areas may help induce electroconvection [Krol et al., 1999]. On the other hand, the increased surface charge density

also strengthens the intensity of electrical field around the ion-exchange membranes. Therefore, the electroconvection effect seemingly becomes more violent as the ε_c values increase. The electric field in the water splitting layer can be estimated by using Poisson's equation [Simons, 1984]:

$$\frac{dE}{dx} = \frac{\rho}{\varepsilon_0 \varepsilon_r}, \tag{4}$$

where E is the electric field intensity (V m^{-1}), x the distance, ρ the space charge density, ε_r the relative permittivity, and ε_0 the vacuum electric permittivity. Assuming that the space charge density is approximately equal to the fixed charge density (N^-), the electric field can be expressed by:

$$E(x) = E(\delta) + \frac{F}{\varepsilon_0 \varepsilon_r}\int_{\delta}^{x} N^- dx, \tag{5}$$

where δ denotes the thickness of the space charge layer. Therefore, the surface charge density is clearly one of the most dominant factors affecting CP behavior. Moreover, increases in the measured LCD values corresponded with increases in the ε_c values. The superficial LCD values are closely related to surface heterogeneity. Lower superficial LCDs indicate that more non-conducing (inert) regions exist on the membrane surface [Rubinstein et al., 1997].

2. Effects of Membrane Surface Properties on Water Splitting (WS)

Water splitting takes place at the interface between the ion-exchange membrane surface and electrolyte solution under the over-LCD condition. To explain the water-splitting mechanism in an ion-exchange membrane, the electric field-enhanced water splitting and catalytic proton transfer reactions were employed [Jialin et al., 1998; Ramírez et al., 1992; Simons, 1979; Strathmann et al., 1997]. When the applied electric field is high enough, Ohm's law is no longer valid. The conductance of electrolytes also increases rapidly with the field [Simons, 1979; Onsager, 1934]. When weak electrolyte solutions are used, this phenomenon is known as the Second Wien Effect (SWE). The following equations show the simple kinetic model for water splitting at the cation-exchange membrane containing sulfonic acid groups as the functional group. The whole reaction can be described as follows [Kemperman (Ed), 2000; Simons, 1979]:

$$H_2O \underset{k_{-1}}{\overset{k_1}{\rightleftharpoons}} H^{\delta+}\cdots{}^{\delta-}OH \underset{k_{-2}}{\overset{k_2}{\rightleftharpoons}} H^+ + OH^- \tag{6}$$

$$H_2O \underset{k_{-1}}{\overset{k_1}{\rightleftharpoons}} H_2O^*_{pair} \qquad \text{Step (1)}$$

$$H_2O^*_{pair} \underset{k_{-2}}{\overset{k_2}{\rightleftharpoons}} H^+ + OH^- \qquad \text{Step (2)}$$

where $H_2O^*_{pair}$ refers to the intermediate (ion pair) for water splitting reaction. The formation of an intermediate is tantamount to the polarization of water molecules at the membrane-solution interface. The forward reaction rate of step (2) is only affected by the intensity of the field [Jialin et al., 1998; Kemperman (Ed), 2000; Simons, 1979]. On the other hand, step (1) is almost completely electrically neutral. Therefore, the water prepolarization step (step (1)) is believed to depend on the membrane surface characteristics (in particular, the fixed charge density). On the other hand, the different water-splitting capabilities of cation exchange membranes can be explained through their varying water prepolarizing tendencies [Jialin et al., 1998]. The reaction rates of the different components, *i.e.*, protons, hydroxyl ions, water ion pairs, and water molecules, are:

$$\frac{dC_{H^+}}{dt} = k_2 C_{H_2O^*_{pair}} - k_{-2} C_{H^+} C_{OH^-} \tag{7}$$

$$\frac{dC_{OH^-}}{dt} = k_2 C_{H_2O^*_{pair}} - k_{-2} C_{H^+} C_{OH^-} \tag{8}$$

$$\frac{dC_{H_2O}}{dt} = k_{-1} C_{H_2O^*_{pair}} - k_1 C_{H_2O} \tag{9}$$

$$\frac{dC_{H_2O^*_{pair}}}{dt} = k_1 C_{H_2O} - k_{-1} C_{H_2O^*_{pair}} + k_{-2} C_{H^+} C_{OH^-} - k_{-2} C_{H_2O^*_{pair}} \tag{10}$$

Assuming the $H_2O^*_{pair}$ formation rate is equal to the removal rate, Eq. (10) can be rewritten as:

$$k_1 C_{H_2O} + k_{-2} C_{H^+} C_{OH^-} = k_{-1} C_{H_2O^*_{pair}} + k_2 C_{H_2O^*_{pair}} = (k_{-1} + k_2) C_{H_2O^*_{pair}} \tag{11}$$

Therefore, the concentration of water ion pairs can be obtained by:

$$C_{H_2O^*_{pair}} = \frac{k_1 C_{H_2O} + k_{-2} C_{H^+} C_{OH^-}}{k_{-1} + k_2}. \tag{12}$$

If the recombination rate of proton and hydroxyl ions is negligible under a strong electric field, the generation rates of these ions are simply described as:

$$\frac{dC_{H^+}}{dt} = \frac{dC_{OH^-}}{dt} = k_2 C_{H_2O^*_{pair}} = \frac{k_1 k_2 C_{H_2O} + k_2 k_{-2} C_{H^+} C_{OH^-}}{k_{-1} + k_2}, \tag{13}$$

$$C_{H^+} = C_{OH^-} = C^*. \tag{14}$$

Likewise, as Simons [Simons, 1979] suggested, the chemical transformation is so fast that the diffusion-controlled process becomes the rate-determining step such that $k_2 \ll k_{-1}$. Therefore, Eq. (13) gives:

$$\frac{dC^*}{dt} = \frac{k_1 k_2}{k_{-1}} C_{H_2O} + \frac{k_2 k_{-2}}{k_{-1}} (C^*)^2. \tag{15}$$

Subsequently, Eq. (15) can be integrated as:

$$C^* = \sqrt{\frac{k_1 C_{H_2O}}{k_{-2}}} \tan\left(\sqrt{\frac{k_1 C_{H_2O}}{k_{-2}}} \frac{k_2 k_{-2}}{k_{-1}} t\right). \tag{16}$$

In Eq. (16), as discussed earlier, the electric field around the membrane surface can affect the rate constant k_2 according to the SWE.

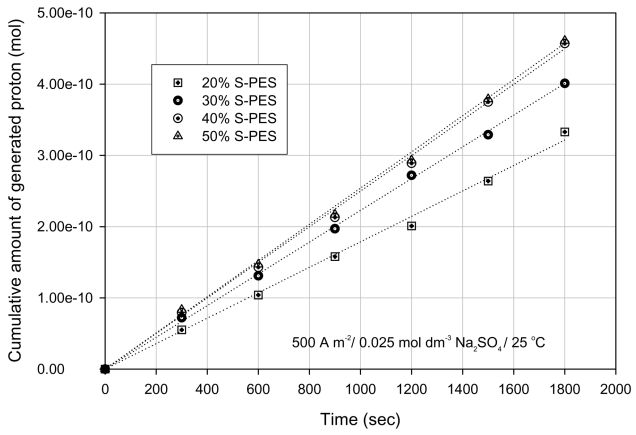

Fig. 5. Cumulative concentrations of generated protons according to time.

Therefore, the differences in water splitting by different cation-exchange membranes are mainly due to differences in the prepolarization effect of water molecules and intensity of the electric field at the solution-membrane interface.

Fig. 5 shows variations in the cumulative concentrations of the protons generated as measured in six-compartment cell experiments. In this figure, the dotted line was obtained from Eq. (16) by plugging typical values obtained from the reference [Simons, 1984]. Note that the calculated results were obtained by varying only the constant k_2. As Simons pointed out, the calculation fits well with the experimental data when the ratio $k_2/(k_{-1}+k_2)$ was less than 10^{-3} [Simons, 1979]. The cumulative concentration of hydroxyl ions shows an approximately linear production in the experimental condition specified, while different slopes were observed for the different membranes. The increasing order of water splitting was 20% S-PES<30% S-PES<40% S-PES<50% S-PES. This sequence corresponds to those of the fractions of the conducting region and apparent surface charge densities shown in Table 1 and Fig. 3, respectively. Therefore, this difference in the water splitting capabilities was seemingly mainly due to their different surface charge densities.

Results of the I-R and chronopotentiometric curves show that with higher fixed charge densities and ε_c values, a more significant electric field was induced. Thus, the prepolarization of water molecules in the membrane-solution interface seems to be enhanced with an increase in the fixed charge density. Meanwhile, stronger electric field can promote more violent water splitting by means of the SWE.

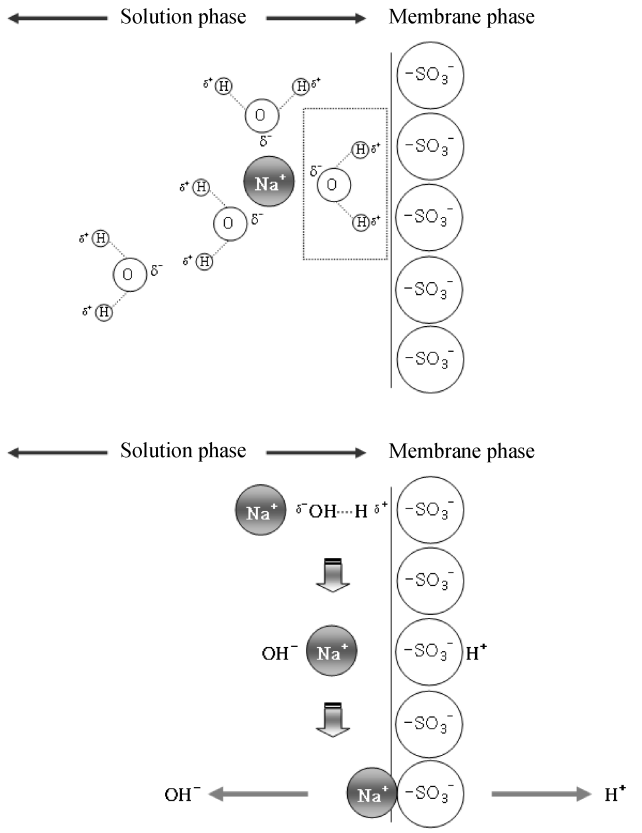

Fig. 6. Schematic drawing of prepolarization of water molecules on the membrane surface.

Apparently, a bipolar structure (like the electrical double layer in the Helmholtz model) was instantly formed at the membrane-solution interface (Fig. 6). As a result, an electrostatic interaction possibly occurs between the fixed ion-exchangeable groups and their hydrated counter ions in the repulsion zone [Patel and Lang, 1977]. In addition, water molecules can be polarized in between with the help of the electric field. However, the bipolar structure may be immediately eliminated due to the electromigration of counter ions through the membrane. Therefore, the unstable electric fields are generated on the interface between the membrane surface and counter ions, thereby promoting electroconvection. This may explain the generation of over-limiting currents and why water splitting in the cation-exchange membrane (*i.e.*, non-fouled membrane) was weaker than that in the membrane with an immobilized bipolar interface (*e.g.*, cation-exchange membranes fouled with metal hydroxides).

3. Effects of Electrolyte Concentration on CP and WS

Fig. 7 shows the I-V and I-R relations measured in NaCl solutions with various ionic concentrations. As the concentration increased, the LCDs also increased according to the classical CP theory. Table 4 lists the characteristic values of the I-R curves. The ΔR and R_{3rd}/R_{1st} values of I-R curves decreased with an increase in the

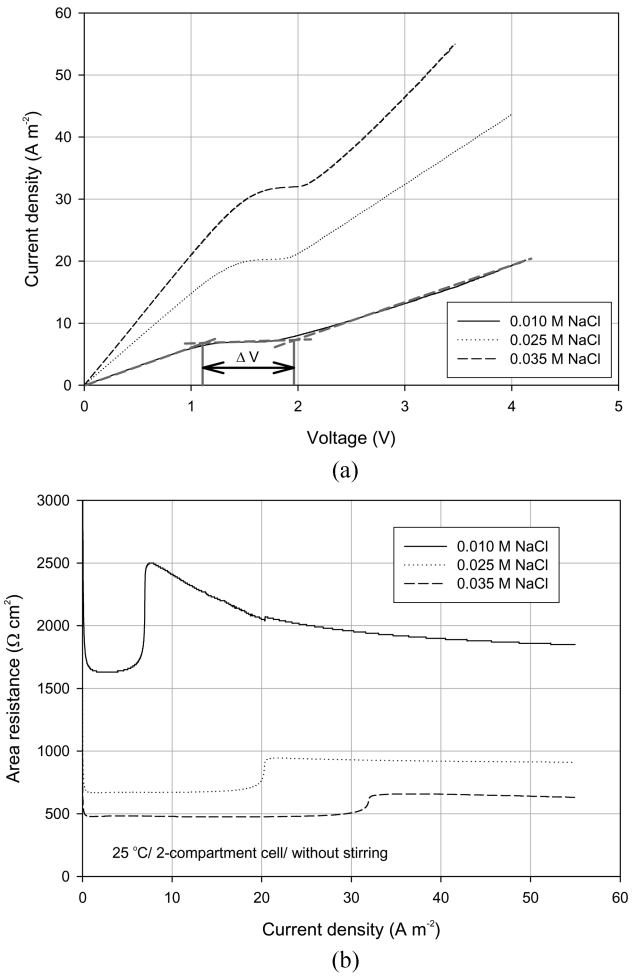

Fig. 7. Current-voltage (I-V) and current-resistance (I-R) curves of CMX membrane contacting with NaCl solution of various concentrations.
(a) Current-voltage curves; (b) Current-resistance curves

Table 4. Characteristic values of I-R curves (CMX membrane)

Electrolyte (NaCl) concentration	0.010 M	0.025 M	0.035 M
R_{1st} (Ω cm^2)	1646.1	672.5	478.2
R_{3rd} (Ω cm^2)	2256.4	923.4	644.4
R_{3rd}/R_{1st} (-)	1.371	1.373	1.347
$R_{inc.}$ (%)	37.1	37.3	34.7
ΔR (Ω cm^2)	610.4	250.9	166.2
LCD (A m^{-2})	6.7	19.9	31.3

ionic concentration.

Several researchers have studied the effects of the electrolytes on CP behavior [Choi et al., 2001a; Rubinstein and Maletzki, 1991]. The contribution of convection to transport relative to diffusion is commonly characterized by the Péclet number Pe [Rubinstein, 1991; Rubinstein and Maletzki, 1991], which is given by:

$$Pe=6\pi(r_o^2 d/\lambda^3), \tag{17}$$

where d is the Stokes radius while λ and r_o are the average interionic distance and Debye length, respectively, which are defined as follows:

$$\lambda=1/(NC_o)^{1/3} \tag{18}$$

$$r_o=\frac{(\varepsilon RT)^{1/2}}{2F(\pi C_o)^{1/2}} \tag{19}$$

From Eqs. (17)-(19),

$$Pe=\frac{3}{2}\left(\frac{\varepsilon RTN}{F^2}d\right), \tag{20}$$

where N is Avogadro's number, C_o the electrolyte concentration, $\varepsilon(=\varepsilon_0\varepsilon_r)$ the dielectric constant, R the gas constant, T the temperature, and F the Faraday constant. From Eq. (20), Pe is clearly independent of the concentration but dependent on the Stokes radius. Pe is proportional to the ionic radius. The plateau length can be expected to decrease with an increase in the Stokes radius of the ion. Therefore, the electrolyte solution containing a larger Stokes radius may have a shorter plateau length [Choi et al., 2001a]. According to Einstein's relation, the Stokes radius of an ion is proportional to the reciprocal of the diffusion coefficient. Thus, the voltage above saturation at which instability commences, *i.e.*, the width of the plateau, depends on the diffusion coefficient of the transported ion. However, this analysis cannot sufficiently explain the difference of the plateau length in the I-V (or I-R) curves measured in different ionic concentrations for the same ion. As the bulk concentration increases, the concentration of ions on the membrane surface also increases. The constant ε in the Debye-Hückel equation is expressed as [Crow, 1994]:

$$\kappa=\left(\frac{e^2\sum N_i z_i^2}{\varepsilon_0\varepsilon_r kT}\right)^{1/2}=\left(\frac{e^2N^2}{\varepsilon_0\varepsilon_r RT}\sum C_i z_i^2\right)^{1/2}, \tag{21}$$

where e is the electronic charge (1.602×10^{-19} A s), N Avogadro's number (6.023×10^{23} mol^{-1}, $N_i=NC_i$), z_i the valence of species i, C_i the concentration of species I (mol dm^{-3}), ε_0 the permittivity of the vacuum (8.85×10^{-12} C^2 J^{-1} m^{-1}), ε_r the relative permittivity (78.54), k the Boltzmann constant (k=R/N), R the gas constant (8.314 J K^{-1} mol^{-1}), and T the temperature (K). Eq. (21) shows that the constant κ increases with an increase in the concentration and charge of ionic species, *i.e.*, increase in the ionic strength μ ($=\frac{1}{2}\sum_i(C_i z_i^2)$). The increase in the constant κ results in the decrease in Debye length r_0 ($=1/\kappa$) and increase in the electrical density ρ according to [Crow, 1994]:

$$\rho=-\kappa^2\phi\varepsilon_0\varepsilon_r, \tag{22}$$

where Φ is the electrostatic potential (V). As a result, the electric field could become stronger in the solution-membrane interface. Therefore, the electroconvective effects could be generated more violently. The width of the plateau region [ΔV in Fig. 7(a)] in the I-V curve decreased with an increase in the constant κ in Eq. (21), as shown in Fig. 8. This could explain the difference in the concentration polarization and water splitting behaviors of ion-exchange membranes coming into contact with an electrolyte of different concentrations.

The relationship between the electrolyte concentration and water splitting property is also presented in Fig. 9. The transport numbers of the hydroxyl ion were observed to increase with an increase in the constant κ. As discussed earlier, this increase is related to the

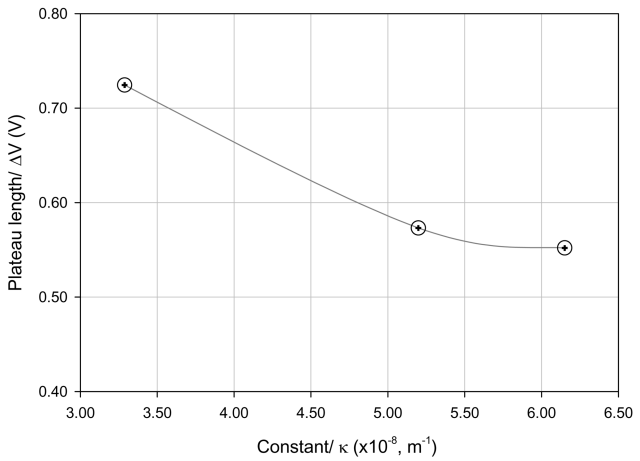

Fig. 8. Variation in plateau lengths (ΔV) of CMX membrane according to the constant κ.

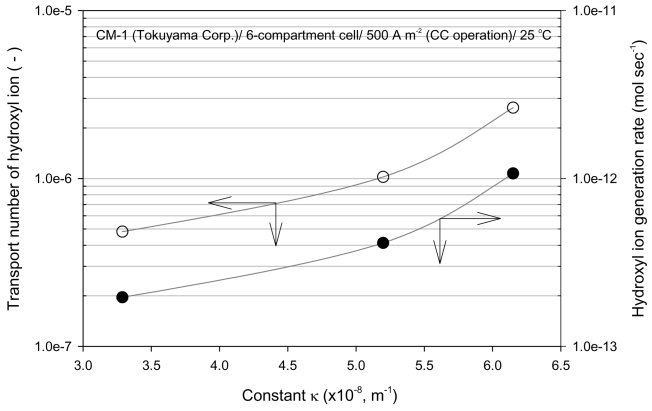

Fig. 9. Variation in water splitting performance of CMX membrane according to the constant κ.

enhancement of electric field and prepolarization of the water molecules through an increase in the density of ionic species coming in contact with the membrane surface. As the salt concentration near the membrane surface increases, the local Debye radius for each ion becomes smaller. This also means that the compensation of counter ions transported out of the solution-membrane interface could be achieved more quickly.

CONCLUSION

The influence of the surface charge density on the polarization and water splitting behaviors was considered. It was observed that the electroconvective effects were closely related with the surface charge density. Based on the results, it was presumed that an increase in the fixed charge density increased the concentration of the counter ions on the membrane surface. Therefore, the electric field around the membrane surface was strengthened in the over-limiting current regions. Water splitting fluxes also increased with an increase in the fixed charge density. This enhancement in water splitting was interpreted in terms of the classical electric field enhanced water splitting theory. Water splitting increased due to the increase in the electric field and prepolarization of water molecules at the membrane-solution interface of the cation-exchange membrane. For the cation-exchange membrane, however, the water splitting effect could be negligible (*i.e.* $t_{H^+}<10^{-5}$) during the electrodialytic operation in an over-LCD condition when the electrolyte solution does not contain multivalent cations. As a result, it could be suggested that cation-exchange membranes with a high surface charge density are more favorable for the electro-membrane process in high current condition due to the more powerful electro-convective effect.

ACKNOWLEDGMENT

This work was supported by the National Research Laboratory (NRL) Program of Korea Institute of Science and Technology Evaluation and Planning (Project No. 2000-N-NL-01-C-185).

REFERENCES

Choi, J.-H. and Moon, S.-H., "Pore Size Characterization of Cation-exchange Membranes by Chronopotentiometry Using Homologous Amine Ions," *J. Membr. Sci*., **191**, 225 (2001).

Choi, J.-H., Lee, H.-J. and Moon, S.-H., "Effects of Electrolytes on the Transport Phenomena in a Cation-exchange Membrane," *J. Colloid & Interf. Sci*., **238**, 188 (2001a).

Choi, J.-H., Kim, S.-H. and Moon, S.-H., "Heterogeneity of Ion-exchange Membranes: The Effects of Membrane Heterogeneity on Transport Properties," *J. Colloid & Interf. Sci*., **241**, 120 (2001b).

Crow, D. R., "Principles and Applications of Electrochemistry," 4th Ed., Blackie Academic & Professional, London (1994).

Jialin, L., Yazhen, W., Changying, Y., Guangdou, L. and Hong, S., "Membrane Catalytic Deprotonation Effects," *J. Membr. Sci*., **147**, 247 (1998).

Jimbo, T., Tanioka, A. and Minoura, N., "Pore-surface Characterization of Poly(Acrylonitrile) Membrane Having Amphoteric Charge Groups by Means of Zeta Potential Measurement," *Colloids and Surface, A*, **159**, 459 (1999).

Kang, M.-S., Choi, Y.-J., Choi, I.-J., Yoon, T.-H. and Moon, S.-H., "Electrochemical Characterization of Sulfonated Poly(arylene ether Sulfone) (S-PES) Cation-Exchange Membranes," *J. Membr. Sci*., **216** (1-2), 39 (2003).

Kang, M.-S., Choi, Y.-J. and Moon, S.-H., "Water Swollen Cation-exchange Membranes Prepared using PVA(polyvinyl Alcohol)/PSSA-MA(polystyrene Sulfonic Acid-co-maleic Acid)," *J. Membr. Sci*., **207**(2), 157 (2002a).

Kang, M.-S., Tanioka, A. and Moon, S.-H., "Effects of Interface Hydrophilicity and MetallIc Compounds on Water Splitting Efficiency in Bipolar Membranes," *Korean J. Chem. Eng*., **19**, 99 (2002b).

Kemperman, A. J. B., "Handbook on Bipolar Membrane Technology," Twente University Press, Enschede (2000).

Kim, Y.-H. and Moon, S.-H., "Lactic Acid Recovery from Fermentation Broth Using One-stage Electrodialysis," *J. Chem. Technol. and Biotechnol*., **176**, 1 (2001).

Krol, J. J., Wessling, M. and Strathmann, H., "Chronopotentiometry and Overlimiting Ion Transport through Monopolar Ion Exchange Membranes," *J. Membr. Sci*., **162**, 155 (1999).

Lee, H.-J., Park, J.-S. and Moon, S.-H., "A Study on Fouling Mitigation Using Pulsing Electric Fields in Electrodialysis of Lactate Containing BSA," *Korean J. Chem. Eng*., **19**, 880 (2002).

Mecham, J., Shobha, H. K., Wang, F., Harrison, W. and McGrath, J. E., "Synthesis and Characterization of Controlled Molecular Weight Sulfonated Aminofunctional Poly(arylene ether sulfone)s Prepared by Direct Polymerization," *Polymer Preprints*, **41**(2), 1388 (2000).

Melnik, L., Vysotskaja, O. and Kornilovich, B., "Boron Behavior During Desalination of Sea and Underground Water by Electrodialysis," *Desalination*, **124**, 125 (1999).

Minagawa, M., Tanioka, A., Ramírez, P. and Mafé, S., "Amino Acid Transport through Cation Exchange Membranes: Effects of pH on Interfacial Transport," *J. Coll. & Interf. Sci*., **188**, 176 (1997).

Montiel, V., García-García, V., González-García, J., Carmona, F. and Aldaz, A., "Recovery by Means of Electrodialysis of an Aromatic Amino Acid from a Solution with a High Concentration of Sulphates and Phosphates," *J. Membr. Sci*., **140**, 243 (1998).

Onsager, L., "Deviation from Ohm's Law in Weak Electrolytes," *J. Chem. Phys.*, **2**, 599 (1934).

Paleologou, M., Wong, P.-Y., Thompson, R. and Berry, R. M., "Bipolar Membrane Electrodialysis for Sodium Hydroxide Production from Sodium Chlorate: Comparison of the Two- and Three-compartment Configurations," *J. Pulp & Paper Sci*., **22**(1), J1 (1996).

Patel, R.-D. and Lang, K.-C., "Polarization in Ion-exchange Membrane Electrodialysis," *Ind. Eng. Chem., Fundam*., **16**(3), 340 (1977).

Ramírez, P., Rapp, H. J., Reichle, S., Strathmann, H. and Mafé, S., "Current-voltage Curves of Bipolar Membranes," *J. Appl. Phys*., **72**(1), 259 (1992).

Rubinstein, I. and Maletzki, F., "Electroconvection at an Electrically Inhomogeneous Permselective Membrane Surface," *J. Chem. Soc. Faraday Trans*., **87**(13), 2079 (1991).

Rubinstein, I., "Electroconvection at an Electrically Inhomogeneous Permselective Interface," *Phys. Fluids*, **3**, 2301 (1991).

Rubinstein, I., Staude, E. and Kedem, O., "Role of the Membrane Surface in Concentration Polarization at Ion-exchange Membrane," *Desalination*, **69**, 101 (1988).

Rubinstein, I., Zaltzman, B. and Kedem, O., "Electric Field in and Around Ion-exchange Membranes," *J. Membr. Sci.*, **125**, 17 (1997).

Sato, K., Sakairi, T., Yonemoto, T. and Tadaki, T., "The Desalination of a Mixed Solution of an Amino Acid and an Inorganic Salt by Means of Electrodialysis with Charge-mosaic Membranes," *J. Membr. Sci*., **100**, 209 (1995).

Shaposhnik, V. A. and Kesore, K., "An Early History of Electrodialysis with Permselective Membranes," *J. Membr. Sci*., **136**, 35 (1997).

Shi, S. and Chen, P.-Q., "Design and Field Trials of a 200 m^3/day Sea Water Desalination by Electrodialysis," *Desalination*, **46**, 191 (1983).

Shim, Y., Lee, H.-J., Lee, S., Moon, S.-H. and Cho, J., "Effects of Natural Organic Matter and Ionic Species on mEmbrane Surface Charge," *Env. Sci. Technol.*, **36**, 3864 (2002).

Simons, R., "Electric Field Effects on Proton Transfer Between Ionizable Groups and Water in Ion-exchange Membranes," *Electrochim. Acta*, **29**, 151 (1984).

Simons, R., "Strong Electric Field Effects on Proton Transfer Between Membrane-bound Amines and Water," *Nature*, **280**, 824 (1979).

Strathmann, H., Krol, J. J., Rapp, H. J. and Eigenberger, G., "Limiting Current Density and Water Dissociation in Bipolar Membranes," *J. Membr. Sci*., **125**, 123 (1997).

Wang, F., Hickner, M., Kim, Y.-S., Zawodzinski, T. A. and McGrath, J. E., "Direct Polymerization of Sulfonated Poly(arylene ether Sulfone) Random (Statistical) Copolymers: Candidates for New Proton Exchange Membranes," *J. Membr. Sci*., **197**, 231 (2002).